

## QUANTIFICATION OF ERRORS IN THE WILSON PLOT APPLIED TO CONDENSATION ON THE OUTSIDE OF TUBES

Bryce M. Burnside<sup>1,\*</sup>, Bodius Salam<sup>2</sup> and David A. McNeil<sup>1</sup>

<sup>1</sup>School of Engineering and Physical Sciences

Heriot-Watt University, Edinburgh, EH14 4AS, UK

<sup>2</sup>Department of Mechanical Engineering

Chittagong University of Engineering and Technology, Chittagong-4349, Bangladesh

\*Corresponding email: B.M.Burnside@hw.ac.uk

**Abstract:** In condensation over horizontal tubes where the wall temperature is not measured directly, the Wilson plot is used to determine the cooling side heat transfer coefficient. Conventionally, the variation in Nusselt number,  $Nu$ , with condensate side temperature drop,  $\Delta T_s$ , which accompanies change of cooling side flowrate, is assumed to be  $Nu \propto 1/\Delta T_s^n$  with  $n = 0.25$ . This is the free convection condensation value. In this paper a technique is devised, not only to check the accuracy of this assumption in the usual vapor side cross flow situation, but also to determine the effect on this accuracy of allowing the index  $n$  to vary. In a case study the best agreement between  $\Delta T_s$  assumed and the value obtained using the cooling side heat transfer coefficient which resulted from the Wilson plot, occurred at  $n = 0.21$ . Based on the random errors in the measured data, a linear regression taking into account the errors in both Wilson plot coordinates gave the cooling side heat transfer coefficient and its uncertainty.

**Keywords:** Heat transfer, condensation, Wilson plots.

### INTRODUCTION

In many laboratory tests or industrial applications, where the vapor side performance of condensing shell and tube heat exchangers is to be determined experimentally, it is not convenient to measure wall temperatures directly. Instead, the Wilson plot is often used to establish the cooling side heat transfer coefficient and hence the vapor side condensate film temperature difference. The technique originated as Wilson's method<sup>1</sup> over 90 years ago. In a steam condenser study, Wilson introduced the plot  $\frac{1}{h_{ov}}$  versus  $\frac{1}{V_{cw}^{0.8}}$ , from the intercept and slope of which the steam side and cooling side heat transfer coefficients may be determined if it is assumed that the steam side coefficient,  $h_s$  can be held constant, while the cooling water velocity is varied. This is impossible to achieve because the condensation film temperature difference,  $\Delta T_s$ , varies with  $V_{cw}$ . To account for this an explicit expression must be found for  $\Delta T_s$  in terms of the heat flux, to allow the reduction of the heat conservation equation to a linear form. For this purpose Briggs and Young<sup>2</sup> introduced the Nusselt expression for condensing heat transfer in natural convection, Eq.(1).

$$Nu_s = A \left\{ \frac{\rho^2 g h_{fg} D^3}{\mu k \Delta T_s} \right\}^{\frac{1}{4}} \quad (1)$$

The Seider-Tate<sup>3</sup> equation accounted for the variation in cooling water properties with  $V_{cw}$  and temperature. They rearranged the Wilson plot coordinates in linear form, so that the values of  $h_{cw}$  and  $A$  could be calculated from the slope and intercept. Recently, Rose<sup>4</sup> revived this modified Wilson plot procedure. Rearranging Eq.(1), the required form, Eq.(2),

$$\Delta T_s = A^{-\frac{4}{3}} \left\{ \frac{\mu D q^4}{\rho^2 g k^3 h_{fg}} \right\}^{\frac{1}{3}} \quad (2)$$

is obtained. By equating heat flux through the wall and writing the overall  $\Delta T_{ov}$  from saturated vapor to cooling water equal to the sum of the temperature differences on the cooling water side, wall and condensate film side, Eq.(3),

$$\Delta T_{ov} = \Delta T_s + \Delta T_w + \Delta T_{cw} \quad (3)$$

two Wilson plot equations,  $Y = f(X)$ , were obtained<sup>4</sup>,

$$Y_1 = aX_1 + b \dots\dots\dots Y_2 = a + bX_2$$

From these, the cooling water side heat transfer coefficient could be evaluated from the intercepts  $b$  and  $a$ , respectively. Rose<sup>4</sup> stated that the two Wilson plots, gave different results.

The aim of this paper is to compare the condensate film temperature difference, implied by Eq.(2) and the value calculated using the cooling water heat transfer coefficient obtained using the Wilson plots. Further, an extra degree of freedom is introduced into Eq.(2) to permit minimization of

**Nomenclature**

$A$	Nusselt Eq. constant, Eq.(1)	$Q_{cw}$	cooling water flow rate, m <sup>3</sup> /s
$a, b$	Wilson plot constants	$Re$	two phase Reynolds number, $Re=\rho VD/\mu, (-)$
$A_{max}$	duct cross-sectional area, m <sup>2</sup>	$T$	temperature, C
$A_{min}$	flow area between tubes, m <sup>2</sup>	$V$	velocity, m/s
$A_{mv}$	mean void area <sup>12</sup> , m <sup>2</sup>	$W_{cw}$	$h_{cw}/C_i$ , kW/m <sup>2</sup> K
$C_i$	$h_{cw}/W_{cw}$	$x$	defined Eq.(5), K
$Con_1$	Eq.(23), ms/K	$X_1, X_2$	Wilson plot parameters, Eqs.(11), (12),(-)
$c_p$	liquid specific heat at constant pressure, kJ/kgK	$y$	defined Eq.(6), K
$D$	tube outside diameter (condensing surface), m	$Y_1, Y_2$	Wilson plot parameters, Eqs.(9), (10),(-)
$D_i$	annulus outside/tube inside diameter, m	$z$	defined Eq.(7), K
$F$	parameter, Eq.(33)	<i>Greek symbols</i>	
$F_1$	Eq.(23), K/ms	$\chi^2$	merit function, Eq.(17)
$G$	parameter, Eq.(33)	$\chi^2_{prob}$	probability of $\chi^2$
$g$	gravitational acceleration, m/s <sup>2</sup>	$\Delta T$	temperature difference, K
$h$	heat transfer coefficient, kW/m <sup>2</sup> K	$\mu$	liquid viscosity, kg/ms
$h_{cw}$	cooling water side heat transfer coefficient <sup>3,6</sup> , kW/m <sup>2</sup> K	$\rho$	liquid density, kg/m <sup>3</sup>
$h_{fg}$	latent heat, kJ/kg	$\sigma$	error
$k$	liquid thermal conductivity, kW/mK	<i>Subscripts</i>	
$L$	effective tube length/pass, m	$cw$	cooling water
$L_{gap}$	minimum gap between tubes, m	$cwi$	cooling water inlet
$K_1$	$\rho_{cw}c_{pcw}/\pi N_{pass}$ , Eq.(20), kW/m <sup>3</sup> K	$cwo$	cooling water outlet
$n$	exponent in Nusselt Eq.(1)	$dat$	Data
$N_{dat}$	number of data points	$lm$	log mean
$N_{pass}$	number of tube passes per row (= 5)	$max$	referring to $A_{max}$
$Nu$	Nusselt number	$min$	referring to $A_{min}$
$P$	parameter, Eq.(32)	$mv$	referring to $A_{mv}$
$p_{tr}$	transverse tube pitch, m	$s$	steam, condensate film
$p_l$	longitudinal tube pitch, m	$sat$	saturation
$q$	heat flux density, tube outside wall, kW/m <sup>2</sup>	$ov$	overall
		$v$	vapor
		$w, wall$	wall

any difference between the two. The study is illustrated by reference to experimental data<sup>5</sup> obtained from the first condensing row of a steam condenser, condensing filmwise, pressure 50 mb, approach velocity  $V_{min}=10$  m/s and heat fluxes 20-90 kW/m<sup>2</sup>. It explores the role of the level of random errors in data measurement on the accuracy of the Wilson plot. The modified Wilson plot method of Rose<sup>4</sup> will first be generalized and the method of linear regression to be used explained. These will be applied in a case study to illustrate the proposed technique.

**WILSON PLOT MODIFIED**

The Rose equations were afforded another degree of freedom by letting the index  $n$  in Eq.(1) vary. Physically this allows for the effect of forced convection on the steam side Nusselt number. Thus, we may write for the more general case.

$$\Delta T_s = A \frac{1}{1-n} \left\{ \frac{\mu D^{\frac{1-3n}{n}} q^{\frac{1}{n}}}{\rho^2 g k^{\frac{1-n}{n}} h_{fg}} \right\}^{\frac{n}{1-n}} \quad (4)$$

Using Rose's notation<sup>4</sup>, write

$$x = \frac{1}{k} \left\{ \frac{\mu D^{\frac{1-3n}{n}} q^{\frac{1}{n}}}{\rho^2 g h_{fg}} \right\}^{\frac{n}{1-n}} \quad (5)$$

$$y = \frac{qD \ln \frac{D}{D_i}}{2k_{wall}} \quad (6)$$

$$z = \frac{qD}{W_{cw} D_i} \quad (7)$$

Here,  $W_{cw}$  is the assumed cooling water heat transfer coefficient calculated using a recommended correlation, eg. Seider and Tate<sup>3</sup> for a circular tube and Gnielinsky<sup>6</sup> for an annulus.  $C_i$  is the correlation factor multiplier of  $W_{cw}$  ( $h_{cw} = C_i W_{cw}$ ) to be determined by the Wilson plot. Thus, from Eq.(3) write

$$\Delta T_{ov} = ax + y + bz \tag{8}$$

Therefore, similarly to Rose<sup>4</sup>, write

$$Y_1 = \frac{\Delta T_{ov} - y}{z} = \frac{\Delta T_{lm} - \frac{qD \ln D/D_i}{2k_{wall}}}{\frac{qD}{W_{cw} D_i}} \tag{9}$$

$$Y_2 = \frac{\Delta T_{ov} - y}{x} = \frac{\Delta T_{lm} - \frac{qD \ln D/D_i}{2k_{wall}}}{\frac{1}{k} \left\{ \frac{\mu D^{1-3n/n} q^{1/n}}{\rho^2 g h_{fg}} \right\}^{n/1-n}} \tag{10}$$

$$X_1 = \frac{x}{z} = \frac{W_{cw} D_i}{qDk} \left\{ \frac{\mu D^{1-3n/n} q^{1/n}}{\rho^2 g h_{fg}} \right\}^{n/1-n} \tag{11}$$

$$X_2 = \frac{z}{x} = \frac{qDk}{W_{cw} D_i} \left\{ \frac{\rho^2 g h_{fg}}{\mu D^{1-3n/n} q^{1/n}} \right\}^{n/1-n} \tag{12}$$

thus the modified Wilson plot Eqs.<sup>4</sup> become Eqs.(13) and (14)

$$Y_1 = aX_1 + b \tag{13}$$

$$Y_2 = a + bX_2 \tag{14}$$

where

$$a = A^{-1/1-n} \tag{15}$$

$$b = \frac{1}{C_i} \tag{16}$$

In each case the error in the slope and intercept of the Wilson plot, caused by experimental uncertainty, is due both to errors in the abscissa and ordinate, X and Y.

**Weighted linear fit caused by errors in both coordinates:**

The problem is to apply a weighted linear fit to linear Eqs.(13) and (14). A Fortran subroutine fitexy<sup>7,8</sup>

fitexy[X, Y, N<sub>dat</sub>, σ(X), σ(Y), a, b, σ(a), σ(b), χ<sup>2</sup>, χ<sup>2</sup><sub>prob</sub>] is used. The input is the N<sub>dat</sub> values, X, Y, above. The output is the best fit to the slope and intercept of the Wilson plot and the errors σ(a) and σ(b), the merit function, χ<sup>2</sup>, and its probability χ<sup>2</sup><sub>prob</sub>. The merit function is defined by Eq.(17)

$$\chi^2(a, b) = \sum_{i=1}^N \left\{ \frac{(Y_i - a - bX_i)^2}{\sigma_{Y_i}^2 + b^2 \sigma_{X_i}^2} \right\} \tag{17}$$

and is the quantity minimized. The denominator of Eq.(17) is the variance of the linear combination  $Y_i - a - bX_i$  of two random variables  $X_i$  and  $Y_i$ <sup>7</sup>, or the inverse of the weights applied to each of the terms in the summation, Eq.(17). It measures the agreement between the data and the straight line model chosen to fit it. Low values of χ<sup>2</sup><sub>prob</sub> indicate a poor fit. Reference<sup>8</sup> shows examples of the use of routine fitexy.

**Measurement data errors-relation to errors in X and Y:**

X and Y are functions of the measured data quantities A,B,C...,X,Y ≡ f(A, B, C...). The errors σ(X) and σ(Y) in X and Y are related to the errors in the experimental data quantities, A, B, C..., σ(A), σ(B), σ(C)...., by the usual relation Eq.(18), for example,

$$\sigma(X) = \sqrt{\left\{ \frac{\partial X}{\partial A} \sigma(A) \right\}^2 + \left\{ \frac{\partial X}{\partial B} \sigma(B) \right\}^2 + \left\{ \frac{\partial X}{\partial C} \sigma(C) \right\}^2 + \text{etc}} \tag{18}$$

The data which is subject to random measurement errors during the Wilson plot tests considered here<sup>5</sup> and the values of these errors, are shown in Table 1. These errors were in effect the random errors of reading the data and an allowance for instability in the experimental conditions during the test.

Table 1: Data measurement errors

Data	σ(data)
Q <sub>cw</sub>	0.005Q <sub>cw</sub> m <sup>3</sup> /s
T <sub>cwi</sub> , T <sub>cwo</sub>	0.02 K
T <sub>sat</sub>	0.1 K

The errors in D, D<sub>i</sub>, L and k<sub>wall</sub> are systematic errors of the Wilson plot tests and are therefore not included in Eq.(18). Obviously these errors, together with the error, here to be estimated, in the cooling water side heat transfer coefficient from the Wilson plot tests, will affect the accuracy of the steam side heat transfer coefficients eventually derived from the main condensation tests. The uncertainty in thermal properties, due to the uncertainty of condensate film and cooling water temperatures, is not included here to avoid difficulties in presentation. However, with obvious modifications it can be. The appropriate average temperature of condensate film and cooling water were used in determining the properties themselves. The object here is to illustrate the general method of assessing the errors involved in the Wilson plot tests and that is not affected by the omission.

**X, Y error differential coefficients:**

Equations (9), (10), (11), and (12) for Y<sub>1</sub>, Y<sub>2</sub>, X<sub>1</sub> and X<sub>2</sub> can be written in terms of the measured data.

First, q must be expressed in terms of the measured quantities

$$q = \frac{K_1 Q_{cw} (T_{cwo} - T_{cwi})}{DL} \quad (19)$$

where

$$K_1 = \frac{\rho_{cw} c_{pcw}}{\pi N_{pass}} \quad (20)$$

Thus, writing q in Eq.(9) in terms of measured data, using Eq.(19),

$$Y_1 = \frac{W_{cw} LD_i \Delta T_{lm}}{K_1 Q_{cw} (T_{cwo} - T_{cwi})} - \frac{D_i W_{cw} \ln D/D_i}{2k_{wall}} \quad (21)$$

In the same way, Eq.(11) becomes

$$X_1 = \text{Con}_1^{n/1-n} F_1^{n/1-n} \frac{W_{cw} D_i}{k} \quad (22)$$

where

$$\text{Con}_1 = \frac{K_1 \mu}{\rho^2 g h_{fg}}; F_1 = \frac{Q_{cw} (T_{cwo} - T_{cwi})}{D^3 L} \quad (23)$$

Similarly for Eqs.(10) and (12) using Eq.(19)

$$Y_2 = \frac{k \Delta T_{lm}}{K_1 D^3 \text{Con}_1^{n/1-n} F_1^{1/1-n}} - \frac{k \ln D/D_i}{2k_{wall} (\text{Con}_1 F_1)^{n/1-n}} \quad (24)$$

$$X_2 = \text{Con}_1^{n/n-1} F_1^{n/n-1} \frac{k}{W_{cw} D_i} \quad (25)$$

Equations (21), (22), (24), and (25) express  $Y_1$ ,  $X_1$  and  $Y_2$ ,  $X_2$  in terms of data values and geometry, all of which are subject to measurement error, as

$$Y_1 \equiv f[Q_{cw}, T_{cwo}, T_{cwi}, T_{sat}] \quad (26)$$

$$X_1 \equiv f[Q_{cw}, T_{cwo}, T_{cwi}, n] \quad (27)$$

and

$$Y_2 \equiv f[Q_{cw}, T_{cwo}, T_{cwi}, T_{sat}, n] \quad (28)$$

$$X_2 \equiv f[Q_{cw}, T_{cwo}, T_{cwi}, n] \quad (29)$$

Note that both  $Y_2$  and  $X_2$  are dependent on n but only  $X_1$  depends on n, not  $Y_1$ . In view of the conditions imposed above, the quantities,  $K_1$  and  $\text{Con}_1$  are

treated as constants. The differential coefficients in the equivalent of Eq.(18) applied to the problem are listed in the Appendix.

**Application:**

The above optimization, Eq.(18), was applied to a data set taken from the first condensing row of a 15 row horizontal steam condenser, titanium tube diameter 19 mm, 0.5 mm thick, described in references<sup>5,9</sup>. Cooling water flowed in the annulus formed by a 14 mm diameter insertion in the tube. The tube configuration was staggered with horizontal and transverse pitches of 25.4 mm. Five tubes formed the row tested. Cooling water flowed through the tubes in series. Each tube was connected by a passage in the tube plates. The temperatures  $T_{cwi}$  and  $T_{cwo}$  were measured at the inlet and outlet of the 5 tube row. The tests were conducted with a vertically downwards inlet steam velocity of 10 m/s, heat fluxes up to 90 kW/m<sup>2</sup> and a pressure of 50 mbar. Index n, Eq.(1) was varied from 0.16 to 0.26,

corresponding to index  $\frac{n}{n-1}$  from 0.19 to 0.35,

Eq.(2). Typically, the resulting values of X and Y and their errors are shown in Tables 2 and 3 for n = 0.25 and 0.21, respectively. Figures 1(a) and (b) show examples of the corresponding modified Wilson plots  $Y = f(X)$ , Eqs.(13) and (14).

Table 4 shows the values of  $C_i$  obtained by the Wilson plots, with un-weighted least squares fits, using Eqs.(13) and (14). As can be seen the difference between the values predicted by the Wilson plots, Eqs.(13) and (14), is only about 0.5%.

The results of the weighted linear regression based on errors in both X and Y, Eqs.(13) and (14) are shown in tables 5 and 6 in the Appendix.  $C_i$  and A were calculated using Eqs.(15) and (16). The probability,  $\chi^2_{prob}$  of  $\chi^2$  is high, particularly at the higher values of n, so that the error in  $C_i$  predicted is

Table 2: Wilson plot, n = 0.25, values of X and Y and errors  $\sigma(X)$  and  $\sigma(Y)$

$\Delta T_{ov}$	$X_1$	$Y_1$	$\sigma(X_1)$	$\sigma(Y_1)$	$X_2$	$Y_2$	$\sigma(X_2)$	$\sigma(Y_2)$
5	0.632	1.466	0.006	0.068	1.582	2.319	0.016	0.124
5	0.472	1.331	0.004	0.055	2.119	2.820	0.019	0.133
5	0.381	1.306	0.003	0.052	2.625	3.429	0.023	0.155
5	0.301	1.239	0.002	0.047	3.327	4.122	0.027	0.176
5	0.554	1.334	0.005	0.059	1.806	2.409	0.017	0.122
10	0.791	1.509	0.005	0.038	1.264	1.908	0.009	0.055
10	0.686	1.442	0.005	0.033	1.457	2.101	0.010	0.057
10	0.558	1.381	0.004	0.030	1.793	2.475	0.011	0.062
10	0.467	1.312	0.003	0.028	2.141	2.809	0.013	0.068
10	0.353	1.224	0.002	0.024	2.835	3.470	0.017	0.179
15	0.840	1.573	0.005	0.027	1.190	1.872	0.007	0.038
15	0.720	1.498	0.004	0.025	1.390	2.082	0.008	0.040
15	0.593	1.427	0.003	0.022	1.687	2.407	0.010	0.043
15	0.507	1.360	0.003	0.020	1.973	2.683	0.011	0.047
15	0.366	1.247	0.002	0.017	2.730	3.404	0.015	0.055

Table 3: Wilson plot,  $n = 0.21$ , values of X and Y and errors  $\sigma(X)$  and  $\sigma(Y)$

$\Delta T_{ov}$	$X_1$	$Y_1$	$\sigma(X_1)$	$\sigma(Y_1)$	$X_2$	$Y_2$	$\sigma(X_2)$	$\sigma(Y_2)$
5	2.383	1.466	0.020	0.068	0.420	0.615	0.004	0.032
5	1.794	1.331	0.014	0.055	0.557	0.742	0.004	0.034
5	1.462	1.306	0.011	0.052	0.684	0.893	0.005	0.039
5	1.165	1.239	0.008	0.047	0.859	1.064	0.006	0.045
5	2.094	1.334	0.017	0.059	0.477	0.637	0.004	0.031
10	2.894	1.509	0.018	0.038	0.351	0.530	0.002	0.015
10	2.481	1.442	0.015	0.033	0.403	0.581	0.002	0.015
10	2.032	1.381	0.012	0.030	0.492	0.679	0.003	0.017
10	1.713	1.312	0.010	0.028	0.584	0.766	0.003	0.018
10	1.307	1.224	0.007	0.024	0.765	0.936	0.004	0.021
15	2.952	1.573	0.017	0.027	0.339	0.533	0.002	0.010
15	2.542	1.498	0.014	0.025	0.393	0.589	0.002	0.011
15	2.108	1.427	0.012	0.022	0.474	0.677	0.003	0.012
15	1.813	1.360	0.010	0.020	0.552	0.750	0.003	0.013
15	1.326	1.247	0.007	0.017	0.754	0.940	0.004	0.015

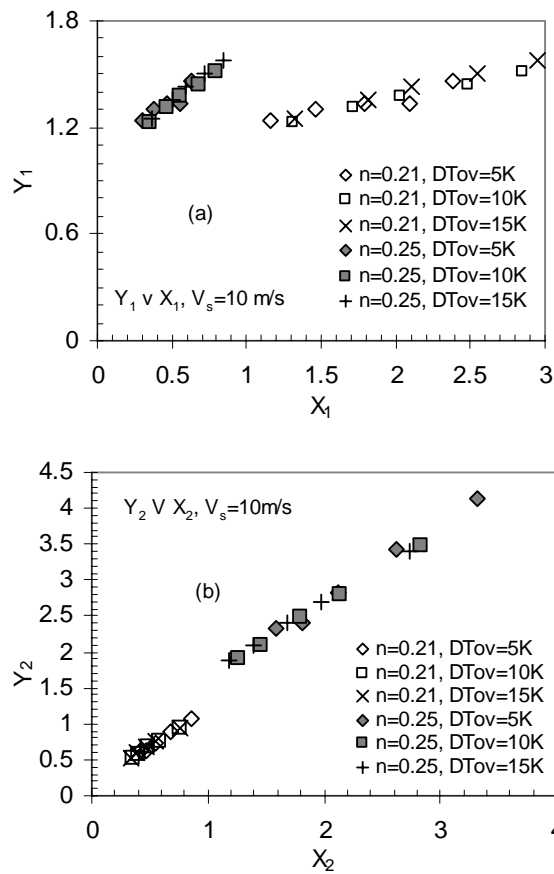


Figure 1: Modified Wilson plots,  $n = 0.21$  and  $0.25$ , (a) Eq.(13) (b) Eq.(14)

acceptable<sup>7</sup>. This implies that the level of random error of the data measurements assumed is reasonable. This assurance is necessary since the random error element arising from instability in conditions during the tests is difficult to determine.

Table 4:  $C_i$  obtained by unweighted Wilson plots,  $n = 0.25$  and  $0.21$

n	$C_i$ , Eq.(14)	$C_i$ , Eq.(15)
0.25	0.971	0.965
0.21	0.992	0.987

Regardless of the value of index  $n$  chosen in the range  $0.16 \leq n \leq 0.26$ , both Wilson plots, give the same values of  $C_i$ . The error in  $C_i$  is  $\pm 3\%$ . The fit, measured by the merit functions  $\chi^2$ , is slightly better using Eq.(14).

What is most notable is that  $C_i$  decreases by about 4% as  $n$  rises from 0.16 to 0.26. This is only slightly more than the estimated error in  $C_i$  itself. It

should be noted that Wilson plot experiments carried out under  $n$  more stable conditions with higher instrument sensitivity would lead to lower values of  $\sigma(C_i)$  therefore increasing the significance of the variation of  $C_i$  with  $n$ .

$\Delta T_s(\text{assumed})$ , based on Eq.(4), with the optimized value of constant  $A$ , was compared with  $\Delta T_s(\text{Wilson plot})$  calculated using  $C_i$  from the Wilson plots. Figure 2(a) shows this comparison for  $n = 0.25$ , optimized coefficients  $A = 1.343$  and  $C_i = 0.994$  (Table 5) based on Eq.(13). The fit for  $n = 0.21$ ,  $A = 3.628$ ,  $C_i = 1.011$  (Table 6) is shown in Fig. 2(c). Figures 2(b) and (d) show the corresponding values for Wilson plot, Eq.(14). Although the agreement shown is excellent, there is a small inherent systematic variation between  $\Delta T_s(\text{assumed})$  and  $\Delta T_s(\text{Wilson plot})$  represented by the inflexion in the data points in the figures. Partly, this is because the power law relationship, Eq.(4) is limited in its ability to represent the experimental

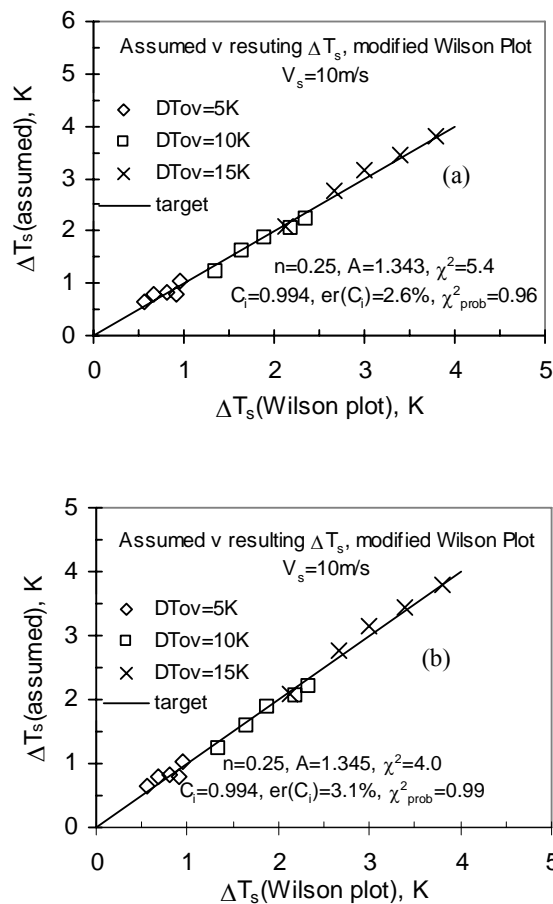


Figure 2: Validity of Eq.(4). (a)  $n=0.25$ , Eq.(13) (b)  $n=0.25$ , Eq.(14) (c)  $n=0.21$ , Eq.(13) (d)  $n=0.21$ , Eq.(14)

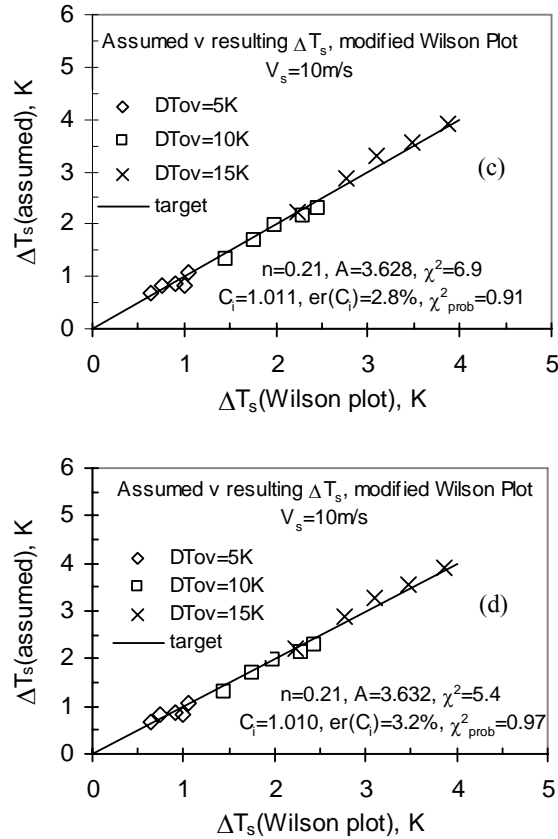


Figure 2(continued): Validity of Eq.(4). (a) n=0.25, Eq.(13) (b) n=0.25, Eq.(14) (c) n=0.21, Eq.(13) (d) n=0.21, Eq.(14)

evidence in forced convection condensation.

The expression, Eq.(30), measures the % difference between  $\Delta T_s(\text{assumed})$  and  $\Delta T_s(\text{Wilson plot})$ .

$$er(\Delta T_s) = 100 \sum_N \left\{ \frac{\Delta T_{sa} - \Delta T_{sc}}{\frac{\Delta T_{sa} + \Delta T_{sc}}{2}} \right\}^2 \quad (30)$$

where  $\Delta T_{sa} = \Delta T_s(\text{assumed})$  and  $\Delta T_{sc} = \Delta T_s(\text{Wilson plot})$

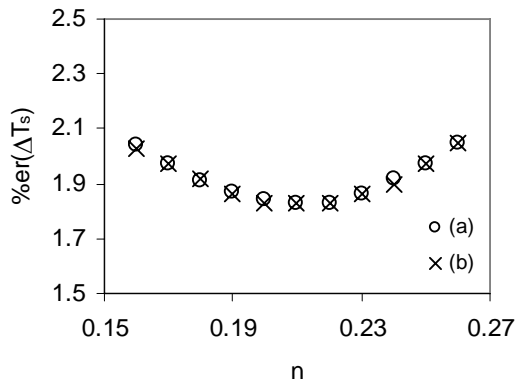


Figure 3: Suitability of Eq.(4) to represent steam side  $\Delta T_s$ , Eq.(13).

plot). Figure 3 shows  $er(\Delta T_s)$  for the whole range of values of  $n$  and for both Wilson plots, Eqs.(13) and (14). The errors are the same for the two plots, but vary with  $n$  from 1.8 to 2.6%, with a minimum value at  $n = 0.21$ .

**Best estimate of  $C_i$ :**

For the set of data used, the value of index  $n = 0.21$  in Eq.(4) best assured that the assumed variation in steam-side heat transfer with heat flux, used in the Wilson plot, corresponded to the value calculated using the derived value of  $C_i$ , Fig.3.  $C_i$  is  $1.01 \pm 3\%$ , Tables 5 and 6. Comparing this value with that at  $n = 0.25$ , the result obtained using the recommended method ( $n = 0.25$ )<sup>2,4</sup>,  $C_i = 0.99 \pm 3\%$ . The comparison is set out in Fig. 4. There is a significant difference of about 2% between the means. The random error in the saturation temperature data considered here,  $\sigma(T_{sat}) = 0.1K$ , is mainly responsible for the uncertainty in  $C_i$ . Reducing it to 0.05K, which was well within the discrimination of the pressure transducer used to determine  $P_{sat}$ , caused  $er(\chi^2_{prob})$  to be unacceptably low. The problem was the scatter of the Wilson plot caused by pressure fluctuations in the rig<sup>10</sup>. The technique described will obviously become more significant when the random errors in the data,

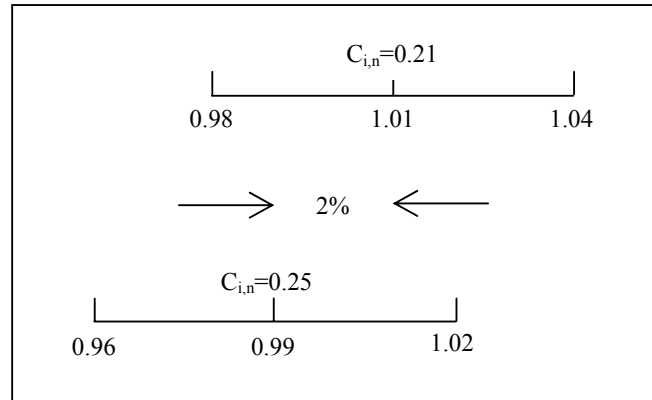


Figure 4: Comparison of recommended Wilson plot technique with present modification

both due to readings errors and fluctuating conditions, are lower. The usefulness of the technique, mainly due to the weighting of errors is not least in the check it affords on the reality of these random error assumptions.

Although they may not be used *a priori* in the analysis, it is interesting to determine the value of *n* which gives the best fit of Rose’s correlations Eqs.(31) and (32)<sup>11</sup>, to Eq.(1). These correlations are recommended as the best fit to data for single tubes and, with the correct choice of equivalent flow area, for bundles of tubes.

$$NuRe^{-1/2} = \frac{0.9(1 + 1/G)^{1/3} + 0.728F^{1/2}}{(1 + 3.44F^{1/2} + F)^{1/4}} \quad (31)$$

For  $P = \frac{\rho_v h_{fg} \mu}{\rho \Delta T_s K} \leq \frac{F}{8}$ , where there is no film separation. Where separation can occur,  $P > \frac{F}{8}$ ,

$$NuRe^{-1/2} = \frac{0.64(1 + 1.81P)^{0.209} (1 + 1/G)^{1/3} + 0.728F^{1/2}}{(1 + 3.51F^{0.53} + F)^{1/4}} \quad (32)$$

with

$$F = \frac{\mu g D h_{fg}}{k V^2 \Delta T_s}; G = \frac{k \Delta T_s}{\mu h_{fg}} \quad (33)$$

*F* and *G*, Eq.(33), allow for the relative effects of gravitational and velocity fields and for the effect of inertia and vapor shear. Equations (31) and (32), were used to calculate *Nu* over the range of  $\Delta T_s$  values, determined by the Wilson plot, for each of the experimental data points at the approach velocity  $V_{max} = 10$  m/s. Separate calculations were carried out for steam velocities, *V*, based on the measured steam mass flowrate and the areas  $A_{min}$ ,  $A_{max}$  and  $A_{mv}$ . The mean void area  $A_{mv}$ , Eq.(34)<sup>12</sup> is given by

$$A_{mv} = L_{gap} \left\{ p_{tr} - \frac{\pi D^2}{4 p_1} \right\} \quad (34)$$

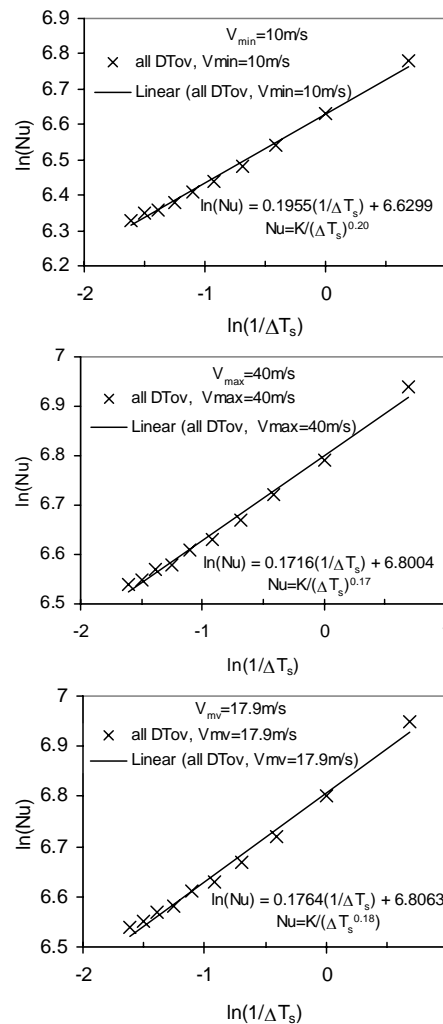


Figure 5:  $\ln(Nu) = f\left(\frac{1}{\Delta T_s}\right)$ , Eqs.(31) and (32), slopes *n*, (a)  $V=V_{min}$ , (b)  $V=V_{max}$ , (c)  $V=V_{mv}$



The calculated velocities were  $V_{\max} = 10$  m/s,  $V_{\min} = 40$  m/s and  $V_{mv} = 17.9$  m/s for the test geometry. The results are shown in a log-log plot in Fig. 5, where the slope  $n$ , is the value which gives the smallest error in matching Eq.(1) to Eqs.(31) or (32). For  $V = V_{\min}$ ,  $n$  is 0.20, for  $V = V_{\max}$ ,  $n = 0.17$  and for  $V = V_{mv}$ ,  $n = 0.18$ . These values are lower than  $n = 0.21$ , the optimum value obtained from the Wilson plots, Fig. 3, but correspond to a negligible difference between  $\Delta T_s$ (assumed) and  $\Delta T_s$ (Wilson plot), Fig.3.

## CONCLUSION

1. This work presents a modification to current methods of applying the Wilson plot to obtain the cooling side heat transfer coefficient. The modification comprises a technique to ensure that the assumed relationship between heat flux and  $\Delta T_s$  on the condensate side is as close as possible to that calculated using the derived cooling side heat transfer coefficient at the test points. This was achieved by allowing the index  $n$  of the conventionally used Nusselt relation for filmwise condensation in natural convection to vary. The values of the Wilson plot coordinates were weighted by the contribution of experimental errors to them.
2. The Wilson plot regression was carried out assuming errors in both coordinates.
3. The two Wilson plots, Eqs. (13) and (14) gave almost identical values of slope and intercept for all values of index  $n$ .
4. For the data studied, the minimum difference between the assumed  $\Delta T_s$  and that calculated using  $C_i$  from the Wilson plot occurred at  $n = 0.21$ . At  $n = 0.25$ , the presently recommended value,  $C_i$  was about 2% lower. The corresponding error in  $C_i$  in both cases was  $\pm 3\%$ . This error was associated rather with fluctuating conditions in the condenser that with errors in instrument readings.
5. The technique is expected to be more significant under steadier condenser conditions and with lower random errors of measurement.

## REFERENCES

- [1] Wilson, E. E., 1915, "A Basis for Rational Design of Heat Transfer Apparatus", Trans. ASME, 37, pp. 47-82.

- [2] Briggs, D. E. and Young, E. H., 1969, "Modified Wilson Plot Techniques for Obtaining Heat Transfer Correlations for Shell and Tube Heat Exchangers", Chem. Eng. Progress Symposium Series, 68(92), pp. 35-45.
- [3] Seider, E. N. and Tate, G. E., 1936, "Heat Transfer and Pressure Drop of Liquids in Tubes", Ind. Eng. Chem., 28, pp. 1429-1435.
- [4] Rose, J. W., 2004, "Heat-transfer Coefficients, Wilson Plots and Accuracy of Thermal Measurements", Exp. Therm. Fluid Sci., 28, pp. 77-86.
- [5] Salam, B., 2004, "Experimental and Numerical Study of Filmwise Condensation of Steam on a Small Tube Bank", PhD Thesis, Heriot-Watt University.
- [6] Gnielinsky, V., 1976, "New Equation for Heat and Mass Transfer in Turbulent Pipe Channel Flow", Int. Chem. Eng., 16(2), pp. 359-368.
- [7] Press, W. H., Teukolsky, S. A., Vetterling, W. T. and Flannery, B. P., 1992, "Numerical Recipes in Fortran", 2<sup>nd</sup> edition, Cambridge University Press.
- [8] Press, W. H., Teukolsky, S. A., Vetterling, W. T. and Flannery, B. P., 1993, "Numerical Recipes Example Book[Fortran]", 2<sup>nd</sup> edition, Cambridge University Press.
- [9] McNeil, D. A., Burnside, B. M. and Cuthbertson, G., 2000, "Dropwise Condensation of Steam on a Small Tube Bank at Turbine Condenser Conditions", Experimental Heat Transfer, 12(2), pp. 89-105.
- [10] Cuthbertson, G., 1999, "An Experimental Investigation of Dropwise and Filmwise Condensation of Low Pressure Steam in Tube Banks", PhD Thesis, Heriot Watt University.
- [11] Rose, J. W., 1984, "Effect of Pressure Gradient in Forced Convection Film Condensation on a Horizontal Tube", Int. J. Heat and Mass Transfer, 27(1), pp. 39-47.
- [12] Nobbs, D. W., 1975, "The Effect of Downward Vapor Velocity and Inundation on the Condensation Rates on Horizontal Tubes and Tube Banks", PhD Thesis, University of Bristol.

**APPENDIX****Derivatives of  $X_1$  and  $Y_1$ :**

$$\frac{\partial X_1}{\partial Q_{cw}} = \frac{n}{1-n} \frac{W_{cw} D_i}{k Q_{cw}} (\text{Con}_1 F_1)^{n/1-n} \quad (36)$$

$$\frac{\partial X_1}{\partial T_{cwo}} = \frac{n}{1-n} \frac{W_{cw} D_i}{k (T_{cwo} - T_{cwi})} (\text{Con}_1 F_1)^{n/1-n} \quad (37)$$

$$\frac{\partial X_1}{\partial T_{cwi}} = -\frac{n}{1-n} \frac{W_{cw} D_i}{k (T_{cwo} - T_{cwi})} (\text{Con}_1 F_1)^{n/1-n} \quad (38)$$

$$\frac{\partial Y_1}{\partial Q_{cw}} = -\frac{\Delta T_{lm} LD_i W_{cw}}{K_1 Q_{cw}^2 (T_{cwo} - T_{cwi})} \quad (39)$$

$$\frac{\partial Y_1}{\partial T_{cwo}} = -\frac{\Delta T_{lm} LD_i W_{cw}}{K_1 Q_{cw} (T_{cwo} - T_{cwi})^2} + \left\{ \frac{\partial \Delta T_{lm}}{\partial T_{cwo}} \right\} \left\{ \frac{LD_i W_{cw}}{K_1 Q_{cw} (T_{cwo} - T_{cwi})} \right\} \quad (40)$$

$$\frac{\partial Y_1}{\partial T_{cwi}} = \frac{\Delta T_{lm} LD_i W_{cw}}{K_1 Q_{cw} (T_{cwo} - T_{cwi})^2} + \left\{ \frac{\partial \Delta T_{lm}}{\partial T_{cwi}} \right\} \left\{ \frac{LD_i W_{cw}}{K_1 Q_{cw} (T_{cwo} - T_{cwi})} \right\} \quad (41)$$

$$\frac{\partial Y_1}{\partial T_{sat}} = \left\{ \frac{\partial \Delta T_{lm}}{\partial T_{sat}} \right\} \left\{ \frac{LD_i W_{cw}}{K_1 Q_{cw} (T_{cwo} - T_{cwi})} \right\} \quad (42)$$

The gradients of  $\Delta T_{lm}$  with respect to  $T_{cwo}$ ,  $T_{cwi}$  and  $T_{sat}$ , given in reference<sup>5</sup>, are repeated below.

$$\frac{\partial \Delta T_{lm}}{\partial T_{cwo}} = \frac{\ln \frac{T_{sat} - T_{cwi}}{T_{sat} - T_{cwo}} - \frac{T_{cwo} - T_{cwi}}{T_{sat} - T_{cwo}}}{\left\{ \ln \frac{T_{sat} - T_{cwi}}{T_{sat} - T_{cwo}} \right\}^2} \quad (43)$$

$$\frac{\partial \Delta T_{lm}}{\partial T_{cwi}} = \frac{-\ln \frac{T_{sat} - T_{cwi}}{T_{sat} - T_{cwo}} + \frac{T_{cwo} - T_{cwi}}{T_{sat} - T_{cwi}}}{\left\{ \ln \frac{T_{sat} - T_{cwi}}{T_{sat} - T_{cwo}} \right\}^2} \quad (44)$$

$$\frac{\partial \Delta T_{lm}}{\partial T_{sat}} = \frac{(T_{cwo} - T_{cwi})^2}{(T_{sat} - T_{cwi})(T_{sat} - T_{cwo})} \frac{1}{\left\{ \ln \frac{T_{sat} - T_{cwi}}{T_{sat} - T_{cwo}} \right\}^2} \quad (45)$$

**Derivatives of  $X_2$  and  $Y_2$ :**

$$\frac{\partial Y_2}{\partial Q_{cw}} = \frac{k}{\text{Con}_1^{n/1-n} Q_{cw}} \left\{ \frac{\Delta T_{lm} F_1^{1/n-1}}{(n-1) K_1 D^3} - \frac{\ln D/D_i}{2k_{wall}} \frac{n}{n-1} F_1^{n/1-n} \right\} \quad (46)$$

$$\frac{\partial Y_2}{\partial T_{cwo}} = k \text{Con}_1^{n/1-n} \left[ \frac{F_1^{1/n-1}}{K_1 D^3} \left\{ \frac{\partial T_{lm}}{\partial T_{cwo}} + \frac{1}{n-1} \frac{\Delta T_{lm}}{(T_{cwo} - T_{cwi})} \right\} - \frac{\ln D/D_i}{2k_{wall}} \left\{ \frac{n}{n-1} \frac{F_1^{n/1-n}}{(T_{cwo} - T_{cwi})} \right\} \right] \quad (47)$$

$$\frac{\partial Y_2}{\partial T_{cwi}} = k \text{Con}_1^{n/1-n} \left[ \frac{F_1^{1/n-1}}{K_1 D^3} \left\{ \frac{\partial T_{lm}}{\partial T_{cwi}} - \frac{1}{n-1} \frac{\Delta T_{lm}}{(T_{cwo} - T_{cwi})} \right\} + \frac{\ln D/D_i}{2k_{wall}} \left\{ \frac{n}{n-1} \frac{F_1^{n/1-n}}{(T_{cwo} - T_{cwi})} \right\} \right] \quad (48)$$

$$\frac{\partial Y_2}{\partial T_{sat}} = \frac{k \text{Con}_1^{n/1-n} F_1^{1/n-1}}{K_1 D^3} \frac{\partial \Delta T_{lm}}{\partial T_{sat}} \quad (49)$$

Since

$$\frac{\partial X_2}{\partial \text{Var}} = -\frac{1}{X_1^2} \frac{\partial X_1}{\partial \text{Var}} \quad (50)$$

where Var is one of  $Q_{cw}$ ,  $T_{cwo}$ ,  $T_{cwi}$ , the appropriate derivatives of  $X_2$  are obtained by multiplying the right hand side of Eqs.(36), (37) and (38) by  $-\frac{1}{X_1^2}$ .

**Fit tables:**Table 5: Wilson plot fit,  $Y_1 = aX_1 + b$ ,  $\sigma(T_{cwo}=T_{cwi}) = 0.02K$ ,  $\sigma(T_{sat}) = 0.10K$ ,  $\sigma(Q_{cw})=0.005Q_{cw}$ 

n	a	b	$\sigma(a)$	$\Sigma(b)$	$\chi^2$	A	$C_i$	$\% \sigma(C_i)$	$\chi^2_{prob}$
0.16	0.049	0.973	0.004	0.029	10.7	12.64	1.028	3.0	0.63
0.17	0.064	0.976	0.005	0.029	9.8	9.843	1.025	3.0	0.71
0.18	0.083	0.979	0.006	0.029	9.0	7.667	1.022	2.9	0.78
0.19	0.110	0.982	0.008	0.028	8.2	5.922	1.018	2.9	0.83
0.20	0.146	0.986	0.010	0.028	7.5	4.654	1.015	2.8	0.87
0.21	0.196	0.989	0.014	0.028	6.9	3.630	1.011	2.8	0.91
0.22	0.264	0.993	0.019	0.028	6.4	2.828	1.007	2.8	0.93
0.23	0.358	0.997	0.025	0.027	6.0	2.206	1.003	2.7	0.95
0.24	0.490	1.001	0.034	0.027	5.7	1.721	0.994	2.7	0.96
0.25	0.675	1.006	0.047	0.027	5.4	1.343	0.994	2.6	0.96
0.26	0.938	1.010	0.066	0.026	5.3	1.048	0.990	2.2	0.97

Table 6: Wilson plot fit,  $Y_2 = a + bX_2$ ,  $\sigma(T_{cwo}=T_{cwi}) = 0.02K$ ,  $\sigma(T_{sat}) = 0.10K$ ,  $\sigma(Q_{cw})=0.005Q_{cw}$ 

n	a	b	$\sigma(a)$	$\Sigma(b)$	$\chi^2$	A	$C_i$	$\% \sigma(C_i)$	$\chi^2_{prob}$
0.16	0.049	0.969	0.004	0.032	9.1	12.55	1.032	3.3	0.77
0.17	0.063	0.977	0.005	0.032	7.7	9.869	1.024	3.3	0.86
0.18	0.084	0.978	0.007	0.032	7.5	7.660	1.022	3.2	0.87
0.19	0.110	0.981	0.009	0.032	6.4	5.959	1.020	3.2	0.93
0.20	0.146	0.985	0.012	0.032	6.0	4.656	1.015	3.2	0.95
0.21	0.195	0.990	0.016	0.032	5.4	3.632	1.010	3.2	0.97
0.22	0.263	0.993	0.021	0.032	5.0	2.831	1.007	3.2	0.98
0.23	0.357	0.998	0.029	0.032	4.5	2.210	1.002	3.2	0.98
0.24	0.488	1.002	0.041	0.031	4.2	1.725	0.998	3.1	0.99
0.25	0.673	1.006	0.057	0.031	4.0	1.345	0.994	3.1	0.99
0.26	0.937	1.011	0.079	0.031	3.9	1.050	0.990	3.1	0.99